JBC RESEARCH ARTICLE

Tumor necrosis factor α upregulates the bile acid efflux transporter OATP3A1 *via* multiple signaling pathways in cholestasis

Received for publication, December 9, 2021 Published, Papers in Press, December 29, 2021,
https://doi.org/10.1016/j.jbc.2021.101543

Mingqiao Li[‡], Weihua Wang[‡], Ying Cheng[‡], Xiaoxun Zhang, Nan Zhao, Ya Tan, Qiaoling Xie, Jin Chai[*], and Qiong Pan[*]

From the Cholestatic Liver Diseases Center and Department of Gastroenterology, Southwest Hospital, Third Military Medical University, Chongqing, China

Edited by Qi Qun Tang

Cholestasis is a common condition in which the flow of bile from the liver to the intestines is inhibited. It has been shown that organic anion–transporting polypeptide 3A1 (OATP3A1) is upregulated in cholestasis to promote bile acid efflux transport. We have previously shown that the growth factor fibroblast growth factor 19 and inflammatory mediator tumor necrosis factor α (TNFα) increased OATP3A1 mRNA levels in hepatoma peritoneal lavage cell/PRF/5 cell lines. However, the mechanism underlying TNFα-stimulated OATP3A1 expression in cholestasis is unknown. To address this, we collected plasma samples from control and obstructive cholestasis patients and used ELISA to detect TNFα levels. We found that the TNFα levels of plasma and hepatic mRNA transcripts were significantly increased in obstructive cholestatic patients relative to control patients. A significant positive correlation was also observed between plasma TNFα and liver OATP3A1 mRNA transcripts in patients with obstructive cholestasis. Further mechanism analysis revealed that recombinant TNFα induced OATP3A1 expression and activated NF-κB and extracellular signal–regulated kinase (ERK) signaling pathways as well as expression of related transcription factors p65 and specificity protein 1 (SP1). Dual-luciferase reporter and chromatin immunoprecipitation assays showed that recombinant TNFα upregulated the binding activities of NF-κB p65 and SP1 to the OATP3A1 promoter in peritoneal lavage cell/PRF/5 cells. These effects were diminished following the application of NF-κB and ERK inhibitors BAY11-7082 and PD98059. We conclude that TNFα stimulates hepatic OATP3A1 expression in human obstructive cholestasis by activating NF-κB p65 and ERK–SP1 signaling. These results suggest that TNFα-activated NF-κB p65 and ERK–SP1 signaling may be a potential target to ameliorate cholestasis-associated liver injury.

Cholestasis is characterized by large amounts of bile acid (BA) accumulation in hepatocytes and serum (1). During an adaptive response to cholestasis, liver injury was attenuated because of the repression of BA synthesis *via* downregulation of *CYP7A1* and *CYP8B1* genes, and the enhancement of BA efflux *via* upregulation of multidrug resistance–associated protein 4, multidrug resistance–associated protein 3 (MRP3), organic anion–transporting polypeptide 3A1 (OATP3A1) protein, bile salt export pump, and organic solute transporter α/β (1–5). These BA transporters played crucial roles in maintaining BA homeostasis. Interestingly, emerging evidence showed that inflammation, as another part of adaptive response for cholestasis, was involved in regulating the expression of BA transporters and liver injury (2, 6). However, the mechanisms how inflammatory factors regulate adaptive expression of BA transporters is unclear.

OATP3A1 (known as *SLCO3A1*) is expressed in multiple tissues (6–12) including the liver and functions as a membrane transporter mediating estrone-3-sulfate, prostaglandins E1 and E2, and thyroxine uptake (12–15). Previously, we have shown that OATP3A1 regulates the transport of BA efflux in cholestasis (6). OATP3A1 knockdown in mice aggravated intrahepatic BA accumulation and cholestatic liver injury (6), indicating that it has a critical role in cholestasis. Moreover, elevation of serum fibroblast growth factor 19 (FGF19) and tumor necrosis factor α (TNFα) has been detected in human obstructive cholestasis (16). We have previously shown that recombinant FGF19 and TNFα stimulated OATP3A1 expression in hepatoma peritoneal lavage cell (PLC)/PRF/5 cell lines, which FGF19 has been proved to upregulate OATP3A1 expression *via* specificity protein 1 (SP1) and NF-κB signaling (6). However, whether and how TNFα regulates OATP3A1 expression in human cholestasis is unclear.

Here, we show that hepatic OATP3A1 is positively correlated with plasma TNFα levels higher in cholestatic patients; further, we identify that TNFα increased OATP3A1 expression by activation of NF-κB p65 and extracellular signal–regulated kinase (ERK)–SP1 signaling. Our data illustrate the molecular mechanism about the upregulation of OATP3A1 induced by TNFα and gain more insight into the significance of OATP3A1 as a potential therapeutic target in cholestasis.

[‡] These authors contributed equally to this study.
[*] For correspondence: Qiong Pan, qiong.pan@cldcsw.org; Jin Chai, jin.chai@cldcsw.org.

Results

The elevation of plasma TNFα levels positively correlated with hepatic OATP3A1 mRNA levels in cholestatic patients

We have found that OATP3A1 levels in hepatic tissues were higher in cholestatic patients compared with control patients (4.8-fold and 3.6-fold higher OATP3A1 protein and mRNA levels, respectively) (6). RT–quantitative real-time PCR (RT–qPCR) analysis showed that liver TNFα mRNA expression in obstructive cholestatic patients was significantly increased relative to the control (Fig. 1*A*). The elevated protein levels and serum levels of TNFα were confirmed in obstructive cholestatic patients (Fig. 1, *B* and *C*), and the linear regression analysis represented that hepatic OATP3A1 expression positively correlated with plasma TNFα levels (Fig. 1*D*). These results indicated that TNFα may contribute to induction of OATP3A1 expression in obstructive cholestatic patients.

Recombinant TNFα stimulated OATP3A1 expression in vitro

Next, we assessed the effect of TNFα-stimulated OATP3A1 expression. Dual-luciferase reporter analysis revealed that both FGF19 and TNFα enhanced *SLCO3A1* promoter activity, and TNFα upregulated the transcriptional activity of the *SLCO3A1* promoter (−2000 to +25 relative to the putative transcription start site) more obviously than FGF19 (Fig. 2*A*), suggesting that TNFα has a vital role in OATP3A1 transcriptional regulation. We treated PLC/PRF/5 cells and primary mouse hepatocytes with recombinant TNFα and found that it increased OATP3A1 expression in a dose-dependent manner. RT–qPCR analysis revealed that treatment with 100 ng/ml TNFα for 24 h, respectively, elevated OATP3A1 mRNA levels by 8.1-fold in primary mouse hepatocytes and 3.2-fold in PLC/PRF/5 cells relative to the control (Fig. 2, *B* and *C*), with no effect on cell viability of PLC/PRF/5 cells (Fig. S1*A*). Meanwhile, RT–qPCR analysis confirmed the similar facilitating effect of TNFα on OATP3A1 upregulation in Huh7 and HepG2 cells (Fig. S1, *B* and *C*). Consistent with this, cell surface protein levels of OATP3A1 were elevated dose-dependently and time-dependently relative to the control (Fig. 2, *D*–*F*). All these results revealed that TNFα could promote the expression of OATP3A1 by increasing the transcriptional activity of *SLCO3A1*.

TNFα increased nuclear NF-κB p65 and SP1 expression and the binding activities of p65 and SP1 to SLCO3A1 promoter

Given that FGF19 induced adaptive expression of OATP3A1 *via* ERK/NFκB–SP1/p65 pathways in cholestatic liver (6), we asked if NF-κB p65 and SP1 promote OATP3A1 transcriptional activity upon TNFα treatment. As expected, the nuclear protein levels of NF-κB p65 and SP1 were enhanced in primary mouse hepatocytes treated by TNFα in a dose-dependent manner (Fig. 3*A*), and these were elevated in PLC/PRF/5 cells in time-dependent and dose-dependent manners (Fig. 3, *B* and *C*). For further determination, *SLCO3A1* promoter deletion-luciferase constructs were generated to identify the *cis*-acting elements respond to NF-κB p65 and SP1 overexpression and TNFα treatment in PLC/PRF/5 cells (Fig. 3*D*). TNFα-induced luciferase activity of the −427

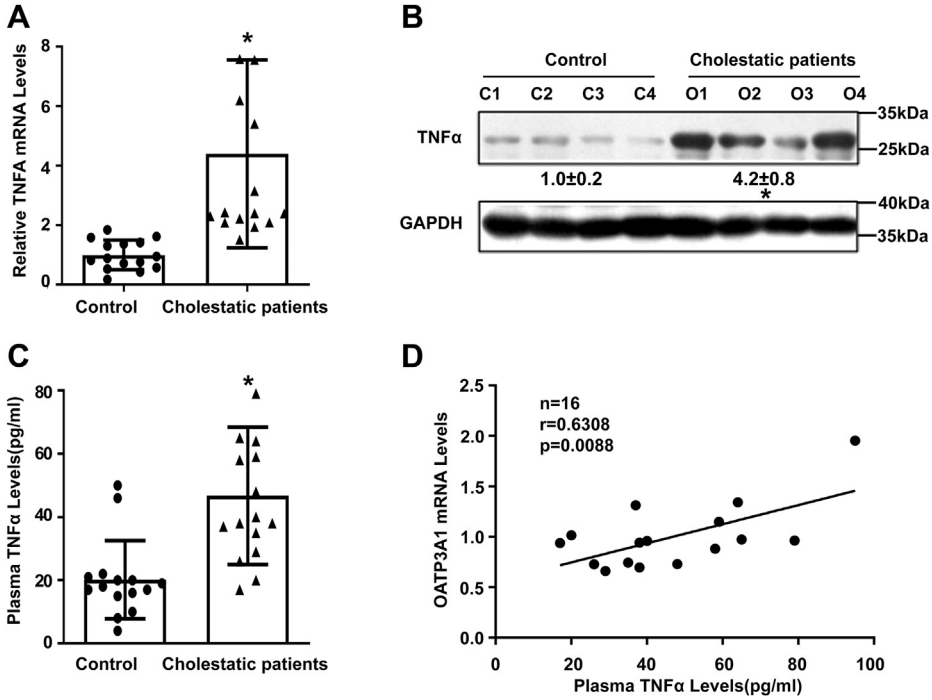

Figure 1. TNFα level is elevated in hepatic tissues of obstructive cholestatic patients (n = 16). *A*, hepatic TNFα mRNA level *versus* the control group (n = 15). *B*, Western blot images for TNFα and their densitometric values were normalized to the control group (C1–4, control; O1–4, obstructive cholestasis livers). *C*, plasma levels of TNFα in cholestatic patients and control. Data are shown as mean ± SD. *$p < 0.05$ *versus* control. The data were analyzed with independent-samples Student's *t* test (two-tailed). *D*, linear regression analysis for plasma TNFα levels and hepatic induction of OATP3A1 mRNA levels in obstructive cholestatic patients (n = 16). OATP3A1, organic anion–transporting polypeptide 3A1; TNFα, tumor necrosis factor α.

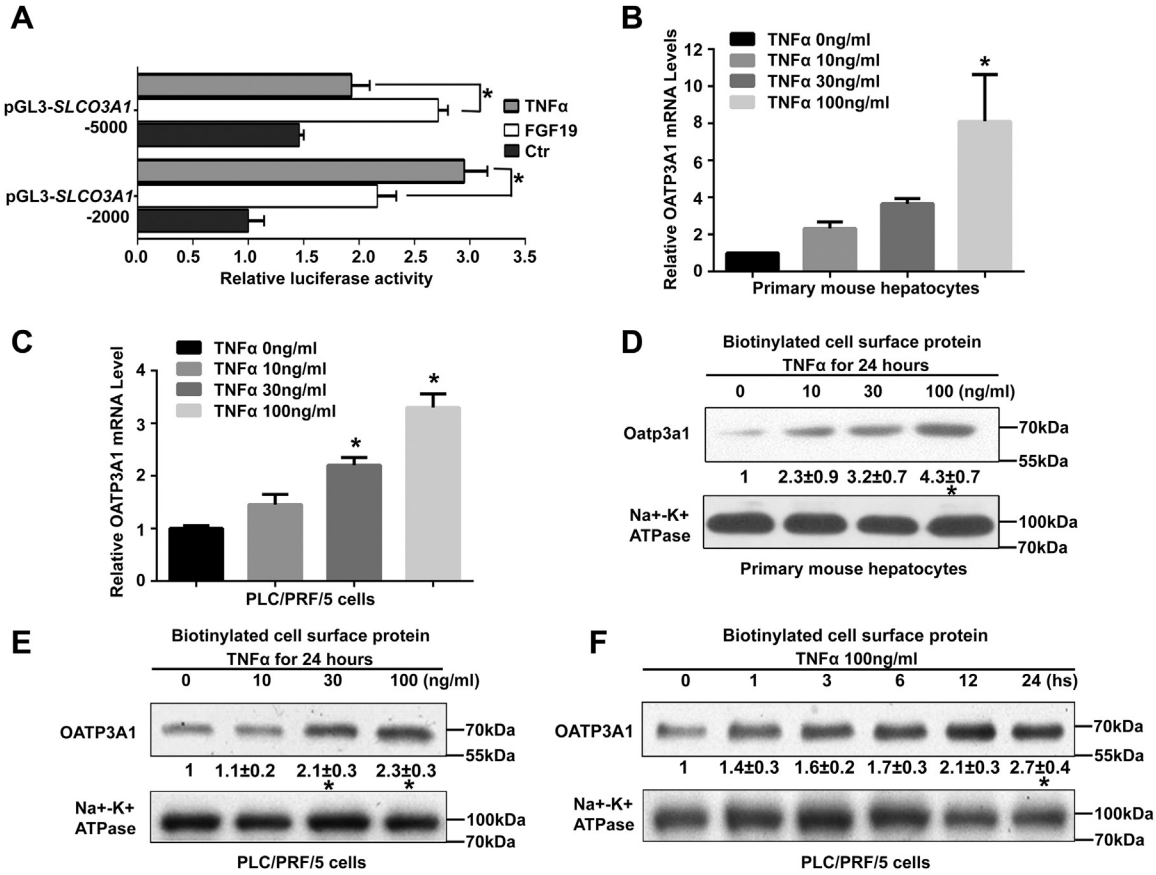

Figure 2. TNFα stimulated OATP3A1 expression in primary mouse hepatocytes and hepatoma PLC/PRF/5 cells. *A*, the different luciferase constructs of *SLCO3A1* promoter were transiently transfected into PLC/PRF/5 cells, which were harvested after 24 h with or without TNFα or FGF19, and relative dual-luciferase activity was determined using a dual-luciferase reporter assay system. *B* and *C*, TNFα-elevated OATP3A1 mRNA levels were detected by RT–qPCR in primary mouse hepatocytes and PLC/PRF/5 cells. *D* and *E*, Western blot analysis for TNFα-elevated biotinylated cell surface OATP3A1 protein levels in primary mouse hepatocytes and PLC/PRF/5 cells. Data are shown as mean ± SD and normalized to expression from control group (0 ng/ml). $*p < 0.05$ *versus* control. The data were analyzed with one-way ANOVA test. FGF19, fibroblast growth factor 19; OATP3A1, organic anion–transporting polypeptide 3A1; PLC, peritoneal lavage cell; qPCR, quantitative PCR; TNFα, tumor necrosis factor α.

to +25 *SLCO3A1* promoter region (pGL3-*SLCO3A1*-427) containing NF-κB p65 *cis*-acting element, respectively, increased by 20-fold and 10-fold in the presence or the absence of NF-κB p65 overexpression, relative to the −183 to +25 *SLCO3A1* promoter region (pGL3-*SLCO3A1*-183) (Fig. 3*E*). In addition, TNFα-induced luciferase activity of the −3478 to +25 *SLCO3A1* promoter region (pGL3-*SLCO3A1*-3478) correspondingly increased by 2.4-fold and 1.6-fold with or without SP1 overexpression, relative to the −2578 to +25 *SLCO3A1* promoter region (pGL3-*SLCO3A1*-2578) (Fig. 3*F*). Taken together, these data indicated that NF-κB p65 *cis*-acting elements located between −427 and −183 contributed to enhanced *SLCO3A1* promoter activity, whereas SP1 *cis*-acting elements situated between −3478 and −2578 of *SLCO3A1* promoter.

To further identify the key sites of NF-κB p65 and SP1 regulating *SLCO3A1* transcription, we performed dual-luciferase reporter assays using mutated NF-κB p65 and SP1 core site plasmids described in our previous study (6). As showed, relative to pGL3-*SLCO3A1*-427 promoter, NF-κB p65 cotransfection with pGL3-*SLCO3A1*-427MUT promoter completely abolished dual-luciferase activity (Fig. 3*G*), whereas cotransfection of pGL3-*SLCO3A1*-3478MUT construct with SP1 reduced dual-luciferase activity by 3.3-fold, compared with pGL3-*SLCO3A1*-3478 promoter (Fig. 3*H*).

Furthermore, chromatin immunoprecipitation (ChIP) assay was used to determine if NF-κB p65 and SP1 could directly interact with potential binding sites on *SLCO3A1* promoter and whether the binding activity of NF-κB p65 and SP1 was enhanced by TNFα treatment. ChIP assay revealed that direct binding activity of NF-κB p65 and SP1 was markedly elevated by TNFα in a dose-dependent manner, representing in ChIP 2-NF-κB p65 site located at −427 to −183 and ChIP 4-SP1 site located at −3478 to −2578, respectively (Fig. 3, *I* and *J*). The TNFα-induced binding activity of these transcription factors was no observable difference relative to the control, respectively, showing in the ChIP 1-NF-κB p65 site located at −643 to −427 and ChIP 3-SP1 site situated at −3689 to −3478 (Fig. 3, *I* and *J*). ChIP assays confirmed that TNFα promotes the direct interaction of NF-κB p65 and SP1 with the *SLCO3A1* promoter. Together, these findings offer solid evidence that TNFα stimulated OATP3A1 expression by upregulating NF-κB p65 and SP1 transcription factors binding to the *cis*-acting elements of *SLCO3A1* promoter.

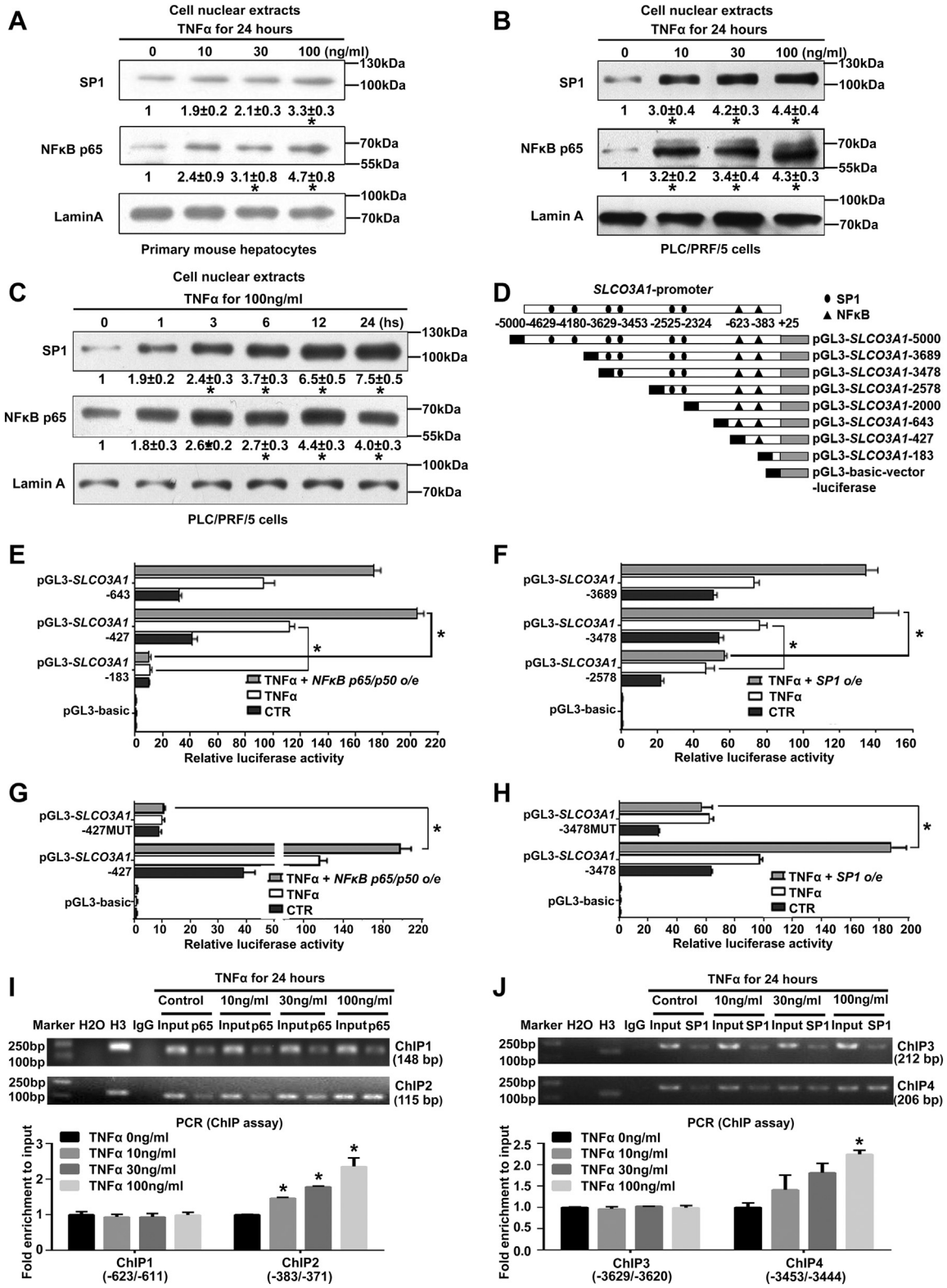

Figure 3. TNFα elevated nuclear protein levels of NF-κB p65 and SP1 as well as p65 and SP1 binding to the *OATP3A1* promoter. *A–C*, TNFα increased SP1 and NF-κB p65 nuclear protein expression dose-dependently and time-dependently in primary mouse hepatocytes and PLC/PRF/5 cells. *D*, the schematic diagram of *SLCO3A1* promoter and construction of deletion mutant luciferase reporter plasmids. *E* and *F*, induction of *SLCO3A1* promoter activity by NF-κB p65 or SP1 constructs was markedly enhanced by TNFα (100 ng/ml). *G* and *H*, dual-luciferase reporter assays for mutated NF-κB p65 and SP1 core site plasmids of the *SLCO3A1* promoter. *I* and *J*, ChIP assay results showed that TNFα elevated NF-κB p65 and SP1 binding to their response elements on the *SLCO3A1* promoter in PLC/PRF/5 cells in a dose-dependent manner. Data are shown as mean ± SD and normalized to the control group (0 ng/ml). *$p < 0.05$ *versus* designated group. The data were analyzed with one-way ANOVA test. ChIP, chromatin immunoprecipitation; OATP3A1, organic anion–transporting polypeptide 3A1; PLC, peritoneal lavage cell; SP1, specificity protein 1; TNFα, tumor necrosis factor α.

TNFα activated NF-κB and ERK signaling in human hepatoma PLC/PRF/5 cells

TNFα engages in several signaling pathways, for example, ERKs and the p38 mitogen-activated protein kinase signaling (17, 18). Our previous work showed that FGF19 induces adaptive OATP3A1 upregulation by activating ERK and NF-κB p65 signaling in cholestatic liver (6). We assessed if NF-κB and ERK signaling are activated by TNFα in PLC/PRF/5 cells. Relative to the control, NF-κB p65 protein phosphorylation in PLC/PRF/5 cells increased upon treatment with TNFα, and similar results were obtained for ERK1/2 phosphorylation (Fig. 4). TNFα promoted NF-κB p65 and ERK1/2 phosphorylation dose-dependently and time-dependently (Fig. 4, *A* and *B*). These results indicated that NF-κB and ERK signaling may be involved in regulation of OATP3A1 induced by TNFα.

TNFα induced OATP3A1 expression through NF-κB and ERK signaling–stimulated nuclear P65 and SP1 expression

To gain further insight into the mechanism underlying OATPA31 regulation by TNFα, we assessed if TNFα–NF-κB/ERK–p65/SP1 signaling can be activated in PLC/PRF/5 cells. Thus, we pretreated cells with BAY 11-7082 (10 μmol/l), an irreversible and selective NF-κB signaling inhibitor, and with PD98059 (25 μmol/l), an ERK signaling blocker, before TNFα treatment. Relative to the control, we found that TNFα alone elevated the cell surface levels of OATP3A1 protein, which was suppressed by pretreatment with BAY 11-7082 or PD98059 in primary mouse hepatocytes and PLC/PRF/5 cells (Fig. 5, *A* and *B*) as well as OATP3A1 mRNA levels in Huh7 and HepG2 cells (Fig. S2, *A* and *B*). Consistent with these changes, TNFα-elevated nuclear protein levels of NF-κB p65 and SP1 were diminished by pretreatment with BAY 11-7082 or PD98059 in primary mouse hepatocytes (Fig. 5*C*). Moreover, NF-κB p65 and ERK1/2 protein phosphorylation was impaired by pretreatment with the NF-κB or ERK inhibitor relative to the TNFα-only treatment in PLC/PRF/5 cells (Fig. 5*D*), and these data further imply the presence of signaling crosstalk between NF-κB and ERK signaling. Therefore, these results delineate that NF-κB signaling mainly promoted TNFα-induced p65 expression, whereas ERK cascades mainly regulated TNFα-stimulated SP1 expression.

To further determine if NF-κB p65 and SP1 *trans*-acting factors could directly bind to *SLCO3A1* promoter, ChIP assays were performed and revealed that TNFα-induced NF-κB p65 (ChIP 2) and SP1 (ChIP 4) binding activities were correspondingly suppressed by the NF-κB inhibitor (BAY 11-7082) and ERK inhibitor (PD98059) (Fig. 5, *E* and *F*), and these data were consistent with the results in Figure 3, *I* and *J*. Thus, our findings showed that TNFα triggered NF-κB p65 and ERK–SP1 signaling pathways and induced transcriptional upregulation of OATP3A1 (Fig. 5*G*).

Discussion

Here, we show a new regulatory mechanism of OATP3A1 in human cholestasis. The three main findings are increased plasma levels of TNFα significantly correlated with OATP3A1 upregulation in livers of obstructive cholestasis patients (Fig. 1*D*); recombinant TNFα elevated OATP3A1 expression in primary mouse hepatocytes and hepatoma cells (Figs. 2, *B–F* and S2); and recombinant TNFα increased p65 and SP1 binding to the *SLCO3A1* promoter *via* NF-κB and ERK signaling pathways (Figs. 3–5).

Cholestasis refers to a spectrum of liver diseases characterized by accumulation of potentially toxic BAs. The impaired BA excretion and homeostasis results in cholestasis-related liver damage (1). In cholestasis, upregulation of BA efflux transporters, for example, MRP3 and OATP3A1 enhance BA elimination by hepatocytes (2–6). OATP3A1 deletion in mice aggravated BA accumulation and cholestatic liver injury, indicating that OATP3A1 has a pivotal role in cholestasis (6). We previously reported that FGF19 stimulates OATP3A1 expression in hepatocytes by activating ERK and NF-κB

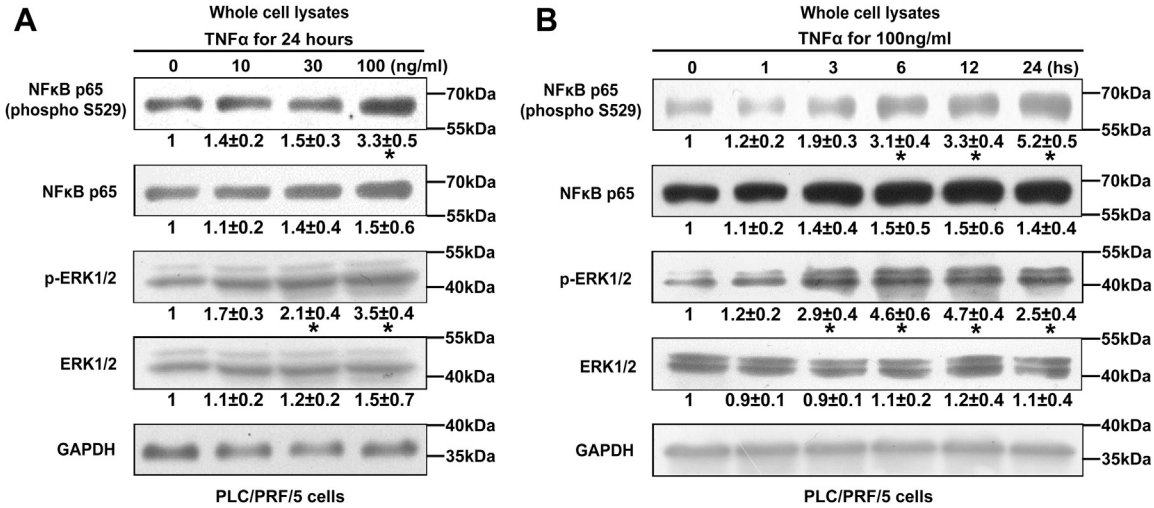

Figure 4. TNFα activated NF-κB and ERK signaling in human hepatoma PLC/PRF/5 cells. *A* and *B*, TNFα increased phosphorylation levels of NF-κB p65 and ERK1/2 dose-dependently and time-dependently. TNFα induced total NF-κB p65 protein expression. Data are shown as mean ± SD and normalized to control group (0 ng/ml). *$p < 0.05$ *versus* control. The data were analyzed with one-way ANOVA test. ERK, extracellular signal–regulated kinase; PLC, peritoneal lavage cell; TNFα, tumor necrosis factor α.

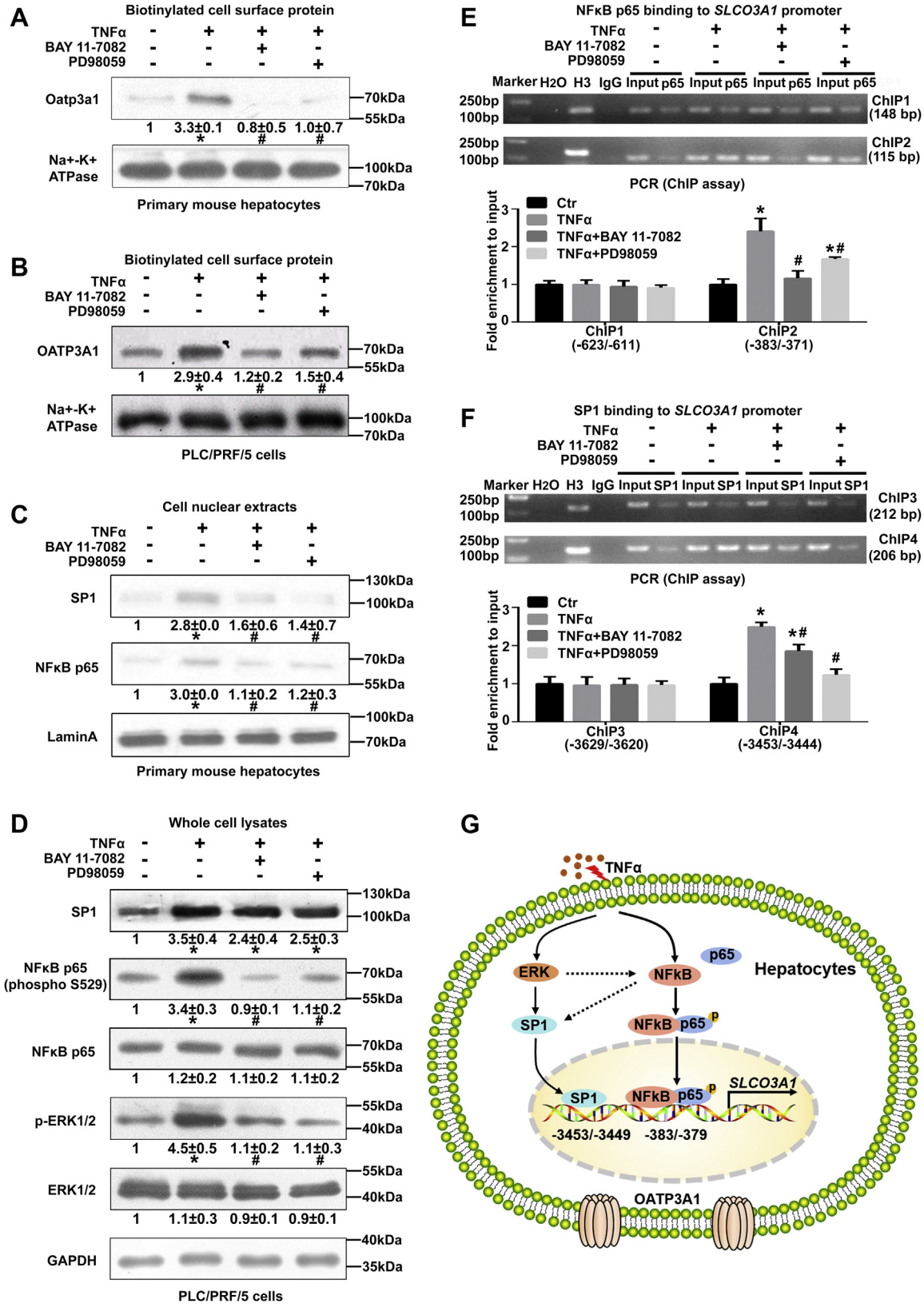

Figure 5. TNFα–NF-κB/ERK–p65/SP1 signaling pathway mediated OATP3A1 expression in PLC/PRF/5 cells and primary mouse hepatocytes treated by TNFα with or without the NF-κB and ERK signaling inhibitors BAY11-7082 (10 μmol/l) and PD98059 (25 μmol/l). *A* and *B*, biotinylated cell surface protein (OATP3A1) was detected by Western blot in primary mouse hepatocytes and PLC/PRF/5 cells, respectively. *C*, Western blot detection of NF-κB p65 and SP1 expression in nuclear extracts of primary mouse hepatocytes. *D*, the expression of phosphorylated NF-κB p65 and SP1 was detected by Western blot in PLC/PRF/5 cells. *E* and *F*, NF-κB p65 and SP1 *cis*-acting elements on *SLCO3A1* promoter were further detected by ChIP assays, and corresponding quantifications were shown below these gels. All experiments were repeated for three times. Data are shown as mean ± SD and normalized to control group without treatment. $^{*}p < 0.05$ *versus* control. $^{\#}p < 0.05$ *versus* TNFα-treated group. The data were analyzed with one-way ANOVA test. *G*, the schematic diagram of the mechanism for TNFα-induced OATP3A1 expression. ChIP, chromatin immunoprecipitation; ERK, extracellular signal–regulated kinase; OATP3A1, organic anion–transporting polypeptide 3A1; PLC, peritoneal lavage cell; SP1, specificity protein 1; TNFα, tumor necrosis factor α.

signaling in cholestasis. We also found that TNFα induced OATP3A1 mRNA expression in hepatoma PLC/PRF/5 cells (6). However, whether and how TNFα promote OATP3A1 levels in hepatic cells in cases of obstructive cholestasis is unclear. Here, we find that elevated levels of plasma TNFα significantly correlate with hepatic OATP3A1 mRNA expression in obstructive cholestasis patients (Fig. 1*D*), indicating that TNFα stimulates hepatic OATP3A1 expression in cholestasis. Further mechanism studies revealed that recombinant TNFα enhanced OATP3A1 protein levels in hepatocytes as well as binding activity of p65 and SP1 to *OATP3A1* promoter (Figs. 2 and 3). Moreover, these alterations were suppressed by the NF-κB and ERK signaling inhibitors, BAY 11-7082 and PD98059, respectively (Fig. 5). These results implied the presence of signaling crosstalk between NF-κB and ERK when TNFα induced transcriptional upregulation of OATP3A1, and it is necessary to further investigate the more details of this mechanism in the adaptive response to cholestasis. Collectively, our findings showed that elevated TNFα levels stimulate hepatic OATP3A1 expression *via* NF-κB and ERK signaling in human obstructive cholestasis. Our findings highlight a novel mechanism of OATP3A1 regulation in cholestasis.

Recent studies show that excessive accumulation of intrahepatic BA triggers inflammatory response by producing inflammatory cytokines and chemokines in the cholestatic liver (19–21). BA accumulation in intestines may activate nuclear receptor farnesoid X receptor and stimulate FGF19 expression (22). BA also stimulates TNFα expression in PLCs (23). Elevated plasma levels of TNFα and FGF19 have been observed in human cholestasis (2, 6). Elevated serum TNFα and FGF19 can target cholestatic liver, repressing BA synthesis through downregulation of CYP7A1 and CYP8B1 expression, and enhancing BA efflux by upregulating MRP3 and OATP3A1 expression (2, 6). Thus, the TNFα and FGF19 elevation may protect from cholestasis. However, FGF19 may cause liver fibrosis by inactivating farnesoid X receptor in human stellate cells (24). High TNFα levels can cause inflammatory injury in inflammatory bowel disease, inflammatory lung disease, and severe alcoholic hepatitis (25–29). Thus, the functional role of TNFα and FGF19 in cholestasis needs further investigation.

In conclusion, we showed that hepatic OATP3A1 levels are upregulated *via* TNFα-mediated activation of NF-κB p65 and ERK–SP1 signaling as a part of an adaptive response to cholestasis. Our findings uncovered a new regulatory mechanism of OATP3A1 as a BA efflux transporter in human cholestasis. Thus, we surmise that TNFα-activated NF-κB p65 and ERK–SP1 signaling may be a potential target to mitigate cholestasis-associated liver injury.

Experimental procedures

Patients and liver sample collection

Ethical approval for the study was granted by the Institutional Ethics Review Committee, Southwest Hospital in Chongqing, China. All patients signed written informed consent. Cholestatic liver samples (n = 16) were collected from patients suspected with periampullary or pancreatic malignancy with severe obstructive cholestasis manifestations. The control group also received liver tissue from patients who underwent liver metastatic resection without cholestasis (n = 15). Clinical features of patients are listed as described previously (6).

Cell culture and treatment

Primary mouse hepatocytes were collected through liver perfusion of C57BL/6J mice with collagenase; human hepatocellular carcinoma PLC/PRF/5, HepG2, and Huh7 hepatocellular carcinoma cell lines were maintained in Dulbecco's modified Eagle's medium supplemented with 10% fetal bovine serum in a 5% CO_2 with 37 °C humidified incubator. Before chemical treatment, the cells were starved by the Dulbecco's modified Eagle's medium with 2% serum (fetal bovine serum) for 12 h, and then TNFα was treated with a gradient concentration (0, 10, 30, and 100 ng/ml), or with 100 ng/ml for 24 h or time gradient (0, 1, 3, 6, 12, and 24 h), inhibitors were pretreated 30 min prior to treatment. TNFα was obtained from PeproTech. PD98059 and BAY 11-7082 were obtained from Sigma–Aldrich. Experiments related to animals were approved by the Institutional Animal Care and Use Committee of the Southwest Hospital affiliated with the Third Military Medical University. Cell viability was assessed by Cell Counting Kit-8 (Genview) according to the manufacturer's protocols.

RNA extraction and RT–qPCR

Total RNA was extracted from liver tissues or cultured cells with Trizol reagent (Invitrogen), then reversely transcribed into complementary DNA (cDNA) with cDNA Synthesis Kit (MBI Fermentas, Inc). The collected cDNA was used for RT–qPCR SYBR premix Ex Taq II Kit (Takara Biotechnology) in a Bio-Rad CFX96. The primer sequences are listed in Table 1, and GAPDH/Gapdh was used as a loading control.

Table 1
Real-time qPCR probes (TaqMan) and primers (SYBR)

Gene	Species/source	Sequences (5′ → 3′)
GAPDH	Human/Hs02758991_g1	Proprietary to ABI
OATP3A1 (*SLCO3A1*)	Human/Hs00203184_m1	Proprietary to ABI
TNFα	Human/Hs01113624_g1	Proprietary to ABI
Gapdh	Mouse/primers (SYBR): NM_001289726.1	Forward: 5′-ACC CTT AAG AGG GAT GCT GC-3′ Reverse: 5′-CGG GAC GAG GAA ACA CTC TC-3′
Oatp3a1 (*Slco3a1*)	Mouse/primers (SYBR): NM_001038643.1	Forward: 5′-CAG TGC CTG CGG AAA AAC TAT-3′ Reverse: 5′-GAC TCA GGG CAG GTT TTC TCT-3′

Table 2
Antibodies used in Western blot (WB) and ChIP

Protein	Host	Company/catalog	Antibody dilution
GAPDH	Rabbit	ProteinTech/10494-1-AP	WB (1:3000)
Na^+/K^+-ATPase	Rabbit	Abcam/ab76020	WB (1:10,000)
OATP3A1 (*SLCO3A1*)	Rabbit	Sigma–Aldrich/SAB1304633	WB (1:1000)
SP1 (H-225)	Rabbit	Santa Cruz/sc-14027	WB (1:1600); ChIP: 2 μg per sample
Phoshpo-ERK1/2	Rabbit	Cell Signaling/#4370	WB (1:2500)
ERK1/2	Rabbit	Cell Signaling/#9102	WB (1:2500)
NF-κB p65 (L8F6)	Mouse	Cell Signaling/#6956	WB (1:1000)
NF-κB p65 (ChIP-grade)	Rabbit	Abcam/ab7970	WB (1:1000); ChIP: 2 μg per sample
Phoshpo-NF-κB p65 (pS529)	Rabbit	Abcam/ab109458	WB (1:2000)
Lamin A	Rabbit	Abcam/ab26300	WB (1:1000)
TNFα	Mouse	BioLegend/#502801	WB (1:1000)

Western blot analysis

The radioimmunoprecipitation assay buffer (Sigma) containing phosphatase and protease inhibitors (Roche) was used for extracting total protein. The commercial kits from Thermo Fisher Scientific were used for extracting nuclear extraction and cell surface protein biotinylation (2). Protein was separated by SDS–PAGE. Primary antibody sources and dilutions are listed in Table 2.

ELISA for detection of TNFα levels in plasma

Plasma samples (control patients, n = 15, and obstructive cholestatic patients, n = 16) were collected before biopsy or hepatectomy using heparin and stored at −80 °C. Levels of TNFα in the collected samples were quantified using TNFα ELISA Kit (BD Biosciences) according to the manufacturer's instructions.

SLCO3A1 *promoter luciferase reporter assays*

Human genetic *SLCO3A1* proximal promoter (−5000 to +25) and its deletion mutants (−3689, −3478, −2578, −643, −427, and −183 to +25) were cloned into pGL3-basic-vector, which contains dual luciferase. Primer sequences are listed in Table 3. The pGL3-*SLCO3A1*-3478MUT and pGL3-*SLCO3A1*-427MUT constructs mutated the key motifs of potential transcriptional factor response elements in the pGL3–3478/+25 and pGL3–427/+25 constructs, respectively. In brief, PLC/PRF/5 cells were transfected with pGL3-*SLCO3A1* plasmids or pGL3-basic-vector plasmids (100 ng) as the control plasmid, NF-κB p65/p50 (100 ng) or SP1 (100 ng) and pRL-TK (10 ng) with Fugene HD transfection reagent (Promega Corporation); for luciferase reporter assay, the pRL-TK plasmid was used as a loading control to standardize the dual-luciferase activity. Then, PLC/PRF/5 cells were treated with TNFα (100 ng/ml) for 24 h after transfection. Passive lysis buffer was used for lysing the treated cells, and Dual-Luciferase Assay Kit (Promega Corporation) was used to measure the dual-luciferase activity.

ChIP assays

ChIP assays were conducted using a commercial ChIP Assay Kit (Millipore) according to the manufacturer's instructions. PLC/PRF/5 cells were used for preparing soluble chromatins. The chromatins were immunoprecipitated using antibodies against SP1 and NF-κB p65 (Table 2). Next, the specified regions containing SP1 or NF-κB p65 binding sites of *SLCO3A1* promoter were amplified with primers described in our previous study (30), which the ChIP1 (−623) and ChIP2 (−383) were for NF-κB p65 binding sites and ChIP3 (−3629) and

Table 3
The primer sequences used for construction of *SLCO3A1* promoter plasmids

pGL3-Dual Luc	Primer pairs
pGL3-*SLCO3A1*-5000	Forward: 5′-CGACGCGT TCA ACA GAA GCA GCA AAT G-3′ Reverse: 5′-GAAGATCT CCG CCG CCG CCG CCG CCG CGA TC-3′
pGL3-*SLCO3A1*-3689	Forward: 5′-CGACGCGT GCT GGG GCT GAG GGG GTG AG-3′ Reverse: 5′-GAAGATCT CCG CCG CCG CCG CCG CCG CGA TC-3′
pGL3-*SLCO3A1*-3478	Forward: 5′-CGACGCGT GCC CCG CAG CGC CAC CTA GG-3′ Reverse: 5′-GAAGATCT CCG CCG CCG CCG CCG CCG CGA TC-3′
pGL3-*SLCO3A1*-2578	Forward: 5′-CGACGCGT AGA GCA CAA CAT CTG TCC CC-3′ Reverse: 5′-GAAGATCT CCG CCG CCG CCG CCG CCG CGA TC-3′
pGL3-*SLCO3A1*-2000	Forward: 5′-CGACGCGT GGC CTC AGT TGT CTC ATC TGT A-3′ Reverse: 5′-GAAGATCT CCG CCG CCG CCG CCG CCG CGA TC-3′
pGL3-*SLCO3A1*-643	Forward: 5′-CGACGCGT TGC CCT TCT CAG TCT GTA CAT G-3′ Reverse: 5′-GAAGATCT CCG CCG CCG CCG CCG CCG CGA TC-3′
pGL3-*SLCO3A1*-427	Forward: 5′-CGACGCGT AGC AAA AGA ACA AAG CTT CC-3′ Reverse: 5′-GAAGATCT CCG CCG CCG CCG CCG CCG CGA TC-3′
pGL3-*SLCO3A1*-183	Forward: 5′-CGACGCGT GGA GGG GGC ACT GCA GTT C-3′ Reverse: 5′-GAAGATCT CCG CCG CCG CCG CCG CCG CGA TC-3′
pGL3-*SLCO3A1*-3478 MUT	Forward: 5′-AGC AAA AGA ACA AAG CTT CCA CAG CAG CTT TTG TTC-3′ Reverse: 5′-GGA CAA ATA AGG GAA CAA AAG CTG CTG TGG AAG-3′
pGL3-*SLCO3A1*-427 MUT	Forward: 5′-GCC TCC CGC CCT CAG TTT CAC CCC CCT TAC T-3′ Reverse: 5′-AGT AAG GGG GGT GAA ACT GAG GGC GGG AGG C-3′

Annotation: The underlined parts in the primers are MluI and BglII adapters.
Abbreviation: MUT, mutant.

Table 4
PCR primers for ChIP assays

ChIP	Primer pairs	Products (bp)
NF-κB ChIP1 (−623)	Forward: 5′-AAG CCT CAA GCA GCT CTG AC-3′ Reverse: 5′-TCA GAG GGC AGG CTG TTC CCA-3′	148
NF-κB ChIP2 (−383)	Forward: 5′-GCG CAG AGC CGC CAG TCT CC-3′ Reverse: 5′-GAC CCG GAG TCC TTG CGG AGT-3′	115
SP1 ChIP3 (−3629)	Forward: 5′-TTT AAG TTG TCG GCT TTC-3′ Reverse: 5′-TAA CAC TCA CCG CAA AGG-3′	212
SP1 ChIP4 (−3453)	Forward: 5′-CCC AAA GAG TGA GTA GCA-3′ Reverse: 5′-GTA AAA ACG CAC CAA TCG-3′	206
ChIP for positive control (GAPDH)	Forward: 5′-TAC TAG CGG TTT TAC GGG CG-3′ Reverse: 5′-TCG AAC AGG AGG AGC AGA GAG CGA-3′	166

ChIP4 (−3453) were for SP1 binding sites. The PCR products were used for agarose gel electrophoresis to detect the levels of *SLCO3A1* promoter motif binding to SP1 and NF-κB p65. The primer sequences are listed in Table 4.

Statistical analysis

The GraphPad Prism (version 6.01) (GraphPad Prism Software) was used for data analysis. Data were shown as mean ± SD and analyzed with one-way ANOVA test and independent-samples Student's t test (two-tailed). $p < 0.05$ indicated statistical significance.

Data availability

All experimental data for this article are available upon e-mail request to Qiong Pan (Southwest Hospital, qiong.pan@cldcsw.org).

Supporting information—This article contains supporting information.

Acknowledgments—This work was supported by the Natural Science Foundation of Chongqing (cstc2019jcyj-msxmX0373) and the National Natural Science Foundation of China (31971086, 81922012, and 81770583).

Author contributions—Q. P. conceptualization; M. L., W. W., and Y. C. methodology; M. L. formal analysis; M. L., W. W., Y. C., X. Z., N. Z., Y. T., and Q. X. resources; W. W. and Y. C. data curation; M. L. writing–original draft; Q. P. and J. C. writing–review & editing; Q. P. and J. C. supervision; Q. P. project administration.

Conflict of interest—The authors declare that they have no conflicts of interest with the contents of this article.

Abbreviations—The abbreviations used are: BA, bile acid; cDNA, complementary DNA; ChIP, chromatin immunoprecipitation; ERK, extracellular signal–regulated kinase; FGF19, fibroblast growth factor 19; MRP3, multidrug resistance–associated protein 3; OATP3A1, organic anion–transporting polypeptide 3A1; PLC, peritoneal lavage cell; RT–qPCR, RT–quantitative real-time PCR; SP1, specificity protein 1; TNFα, tumor necrosis factor α.

References

1. Cai, S. Y., and Boyer, J. L. (2019) Bile infarcts: New insights into the pathogenesis of obstructive cholestasis. *Hepatology* **69**, 473–475
2. Chai, J., He, Y., Cai, S. Y., Jiang, Z., Wang, H., Li, Q., Chen, L., Peng, Z., He, X., Wu, X., Xiao, T., Wang, R., Boyer, J. L., and Chen, W. (2012) Elevated hepatic multidrug resistance-associated protein 3/ATP-binding cassette subfamily C 3 expression in human obstructive cholestasis is mediated through tumor necrosis factor alpha and c-Jun NH2-terminal kinase/stress-activated protein kinase-signaling pathway. *Hepatology* **55**, 1485–1494
3. Chai, J., Cai, S. Y., Liu, X., Lian, W., Chen, S., Zhang, L., Feng, X., Cheng, Y., He, X., He, Y., Chen, L., Wang, R., Wang, H., Boyer, J. L., and Chen, W. (2015) Canalicular membrane MRP2/ABCC2 internalization is determined by Ezrin Thr567 phosphorylation in human obstructive cholestasis. *J. Hepatol.* **63**, 1440–1448
4. Chai, J., Luo, D., Wu, X., Wang, H., He, Y., Li, Q., Zhang, Y., Chen, L., Peng, Z. H., Xiao, T., Wang, R., and Chen, W. (2011) Changes of organic anion transporter MRP4 and related nuclear receptors in human obstructive cholestasis. *J. Gastrointest. Surg.* **15**, 996–1004
5. Zhang, A., Jia, Y., Xu, Q., Wang, C., Liu, Q., Meng, Q., Peng, J., Sun, H., Sun, P., Huo, X., and Liu, K. (2016) Dioscin protects against ANIT-induced cholestasis via regulating Oatps, Mrp2 and Bsep expression in rats. *Toxicol. Appl. Pharm.* **305**, 127–135
6. Pan, Q., Zhang, X., Zhang, L., Cheng, Y., Zhao, N., Li, F., Zhou, X., Chen, S., Li, J., Xu, S., Huang, D., Chen, Y., Li, L., Wang, H., Chen, W., *et al.* (2018) Solute carrier organic anion transporter family member 3A1 is a bile acid efflux transporter in cholestasis. *Gastroenterology* **155**, 1578–1592.e16
7. Roth, M., Obaidat, A., and Hagenbuch, B. (2012) OATPs, OATs and OCTs: The organic anion and cation transporters of the SLCO and SLC22A gene superfamilies. *Br. J. Pharmacol.* **165**, 1260–1287
8. Atilano-Roque, A., and Joy, M. S. (2017) Characterization of simvastatin acid uptake by organic anion transporting polypeptide 3A1 (OATP3A1) and influence of drug-drug interaction. *Toxicol. In Vitro* **45**, 158–165
9. Wei, S. C., Tan, Y. Y., Weng, M. T., Lai, L. C., Hsiao, J. H., Chuang, E. Y., Shun, C. T., Wu, D. C., Kao, A. W., Chuang, C. S., Ni, Y. H., Shieh, M. J., Tung, C. C., Chen, Y., Wang, C. Y., *et al.* (2014) SLCO3A1, a novel crohn's disease-associated gene, regulates nf-kappaB activity and associates with intestinal perforation. *PLoS One* **9**, e100515
10. Patel, P., Weerasekera, N., Hitchins, M., Boyd, C. A., Johnston, D. G., and Williamson, C. (2003) Semi quantitative expression analysis of MDR3, FIC1, BSEP, OATP-A, OATP-C,OATP-D, OATP-E and NTCP gene transcripts in 1st and 3rd trimester human placenta. *Placenta* **24**, 39–44
11. Rumiato, E., Brunello, A., Ahcene-Djaballah, S., Borgato, L., Gusella, M., Menon, D., Pasini, F., Amadori, A., Saggioro, D., and Zagonel, V. (2016) Predictive markers in elderly patients with estrogen receptor-positive breast cancer treated with aromatase inhibitors: An array-based pharmacogenetic study. *Pharmacogenomics J.* **16**, 525–529
12. Huber, R. D., Gao, B., Sidler Pfandler, M. A., Zhang-Fu, W., Leuthold, S., Hagenbuch, B., Folkers, G., Meier, P. J., and Stieger, B. (2007) Characterization of two splice variants of human organic anion transporting polypeptide 3A1 isolated from human brain. *Am. J. Physiol. Cell Physiol.* **292**, C795–C806
13. Durmus, S., van Hoppe, S., and Schinkel, A. H. (2016) The impact of Organic Anion-Transporting Polypeptides (OATPs) on disposition and

toxicity of antitumor drugs: Insights from knockout and humanized mice. *Drug Resist. Updat.* **27**, 72–88
14. Adachi, H., Suzuki, T., Abe, M., Asano, N., Mizutamari, H., Tanemoto, M., Nishio, T., Onogawa, T., Toyohara, T., Kasai, S., Satoh, F., Suzuki, M., Tokui, T., Unno, M., Shimosegawa, T., *et al*. (2003) Molecular characterization of human and rat organic anion transporter OATP-D. *Am. J. Physiol. Renal Physiol.* **285**, F1188–1197
15. Bakos, E., Tusnady, G. E., Nemet, O., Patik, I., Magyar, C., Nemeth, K., Kele, P., and Ozvegy-Laczka, C. (2020) Synergistic transport of a fluorescent coumarin probe marks coumarins as pharmacological modulators of organic anion-transporting polypeptide, OATP3A1. *Biochem. Pharmacol.* **182**, 114250
16. Schaap, F. G., van der Gaag, N. A., Gouma, D. J., and Jansen, P. L. (2009) High expression of the bile salt-homeostatic hormone fibroblast growth factor 19 in the liver of patients with extrahepatic cholestasis. *Hepatology* **49**, 1228–1235
17. Tapryal, N., Shahabi, S., Chakraborty, A., Hosoki, K., Wakamiya, M., Sarkar, G., Sharma, G., Cardenas, V. J., Boldogh, I., Sur, S., Ghosh, G., and Hazra, T. K. (2021) Intrapulmonary administration of purified NEIL2 abrogates NF-kappaB-mediated inflammation. *J. Biol. Chem.* **296**, 100723
18. Sabio, G., and Davis, R. J. (2014) TNF and MAP kinase signalling pathways. *Semin. Immunol.* **26**, 237–245
19. Saito, J. M., and Maher, J. J. (2000) Bile duct ligation in rats induces biliary expression of cytokine-induced neutrophil chemoattractant. *Gastroenterology* **118**, 1157–1168
20. Gujral, J. S., Farhood, A., Bajt, M. L., and Jaeschke, H. (2003) Neutrophils aggravate acute liver injury during obstructive cholestasis in bile duct-ligated mice. *Hepatology* **38**, 355–363
21. Cai, S. Y., Ouyang, X., Chen, Y., Soroka, C. J., Wang, J., Mennone, A., Wang, Y., Mehal, W. Z., Jain, D., and Boyer, J. L. (2017) Bile acids initiate cholestatic liver injury by triggering a hepatocyte-specific inflammatory response. *JCI Insight* **2**, e90780
22. Ding, L., Yang, L., Wang, Z., and Huang, W. (2015) Bile acid nuclear receptor FXR and digestive system diseases. *Acta Pharm. Sin. B* **5**, 135–144
23. Hassoun, E. A., Spildener, J., and Cearfoss, J. (2010) The induction of tumor necrosis factor-alpha, superoxide anion, myeloperoxidase, and superoxide dismutase in the peritoneal lavage cells of mice after prolonged exposure to dichloroacetate and trichloroacetate. *J. Biochem. Mol. Toxicol.* **24**, 136–144
24. Schumacher, J. D., Kong, B., Wu, J., Rizzolo, D., Armstrong, L. E., Chow, M. D., Goedken, M., Lee, Y. H., and Guo, G. L. (2020) Direct and indirect effects of fibroblast growth factor (FGF) 15 and FGF19 on liver fibrosis development. *Hepatology* **71**, 670–685
25. Griffiths, O. R., Landon, J., Coxon, R. E., Morris, K., James, P., and Adams, R. (2020) Inflammatory bowel disease and targeted oral anti-TNFalpha therapy. *Adv. Protein Chem. Struct. Biol.* **119**, 157–198
26. Malaviya, R., Laskin, J. D., and Laskin, D. L. (2017) Anti-TNFalpha therapy in inflammatory lung diseases. *Pharmacol. Ther.* **180**, 90–98
27. Bradham, C. A., Plumpe, J., Manns, M. P., Brenner, D. A., and Trautwein, C. (1998) Mechanisms of hepatic toxicity. I. TNF-induced liver injury. *Am. J. Physiol.* **275**, G387–G392
28. Bird, G. L., Sheron, N., Goka, A. K., Alexander, G. J., and Williams, R. S. (1990) Increased plasma tumor necrosis factor in severe alcoholic hepatitis. *Ann. Intern. Med.* **112**, 917–920
29. Mookerjee, R. P., Sen, S., Davies, N. A., Hodges, S. J., Williams, R., and Jalan, R. (2003) Tumour necrosis factor alpha is an important mediator of portal and systemic haemodynamic derangements in alcoholic hepatitis. *Gut* **52**, 1182–1187
30. Pan, Q., Tian, Y., Li, X., Ye, J., Liu, Y., Song, L., Yang, Y., Zhu, R., He, Y., Chen, L., Chen, W., Mao, X., Peng, Z., and Wang, R. (2013) Enhanced membrane-tethered mucin 3 (MUC3) expression by a tetrameric branched peptide with a conserved TFLK motif inhibits bacteria adherence. *J. Biol. Chem.* **288**, 5407–5416